Saudi Pharmaceutical Journal (2025) 33:8
https://doi.org/10.1007/s44446-025-00009-3

RESEARCH ARTICLE

Exosomes derived from umbilical cord blood NK cells inhibit the progression of pancreatic cancer by targeting ROS-mediated mitochondrial dysfunction

Yanyun Zheng[1] · Xinfeng Zou[2] · Qun Li[1] · Dongjun Jiang[1] · Feng Zhu[1] · Yanqun Wu[1]

Received: 5 February 2025 / Accepted: 31 March 2025 / Published online: 29 April 2025

Abstract

Emerging research indicates that natural killer (NK) cell-derived exosomes (NK-exo) play a significant role in cancer development. However, their regulatory mechanisms, particularly in pancreatic cancer, remain poorly elucidated. This study employed an in vitro co-culture system and an in vivo subcutaneous tumor model to evaluate the anti-tumor effect of NK-exo on pancreatic cancer. Umbilical cord blood (UCB)-derived NK-exo displayed characteristic exosomal morphology, size, and marker expression and was internalized by PANC- 1 cells. NK-exo significantly and dose-dependently reduce cell proliferation, migration, and invasion ($P < 0.01$). Further analysis demonstrated that NK-exo induced mitochondrial apoptosis in PANC- 1 cells by altering reactive oxygen species (ROS, $P < 0.0001$) and mitochondrial membrane potential (MPP) levels ($P < 0.0001$), effects that were significantly diminished with N-acetylcysteine (NAC) treatment ($P < 0.0001$). Furthermore, NK-exo treated PANC- 1 cells showed upregulation of the apoptotic markers *Caspase3* ($P < 0.0001$) and *Caspase9* ($P = 0.0086$) and reduced the release of *PGC- 1α* ($P = 0.0064$), *TFAM* ($P < 0.0001$), and *SOD2* ($P = 0.0021$) as demonstrated by qRT-PCR. Western blot analyses revealed a dose dependent significant elevation of total Caspase3, Caspase9, Bax, and cytochrome c level and depression in the anti-apoptotic Bcl- 2. Animal experiments further confirmed that NK-exo treatment significantly reduced tumor volume and weight and increased Bax protein expression relative to the tumor model group. These findings indicate that NK-exo can enter PANC- 1 cells via endocytosis, induce mitochondrial oxidative damage, and suppress PANC- 1 cell progression, thereby demonstrating a robust anti-pancreatic cancer effect.

Keywords Umbilical cord blood · NK cells · Exosomes · Pancreatic cancer · Mitochondrial oxidative damage

1 Introduction

Pancreatic cancer is an aggressive tumor with high rates of metastasis and recurrence, resulting in a poor prognosis. Based on GLOBOCAN 2022 data, there were approximately 510,000 newly diagnosed cases of pancreatic cancer and 467,000 associated mortalities worldwide in 2022. By 2030, it is predicted to represent the leading contributor to cancer-associated mortality in the world. Despite recent therapeutic advancements, the five-year survival rate remains below 10%, primarily due to ineffective early diagnosis and limited targeted therapies (Zhang et al. 2023). Identifying effective treatments for pancreatic cancer remains a significant clinical challenge, requiring the exploration of innovative therapeutic strategies.

Immunotherapy has emerged as a promising approach for cancer treatment. NK cells, a critical component of the immune system, serve as a primary defense against infections and aberrant cells (Hosseini et al. 2022). NK cells show significant potential in cancer immunotherapy by releasing perforin, granzyme and granulysin, as well as activating death receptors (Sordo-Bahamonde et al. 2020). Moreover, NK cells secrete cytokines that mature dendritic cells, activate macrophages, and enhance adaptive immune responses, thereby amplifying anti-tumor immunity (Yu. 2023). However, the ability of NK cells to recognize and destroy tumor cells is significantly reduced in individuals with cancer due

Yanyun Zheng and Xinfeng Zou equally contributed to this work.

✉ Yanqun Wu
yqwu@mail.jnmc.edu.cn

[1] School of Life Science, Jining Medical University, Rizhao City, Shandong, China

[2] Shandong Xinchao Biotechnology Co., Ltd., Rizhao City, Shandong, China

to their inhibition and dysfunction, enabling tumor cells to evade immune surveillance. Therefore, the clinical application of NK cells in cancer therapy remains limited (Zheng et al. 2023).

Exosomes, nanoscale extracellular vesicles secreted by cells, possess a phospholipid bilayer structure and diameters ranging from 30 to 150 nm (Chen et al. 2018; Ren et al. 2022). These vesicles facilitate cell-to-cell communication and have attracted much attention in tumor therapy research as they are associated with minimal risks of malignant transformation and their ability to traverse the blood–brain barrier (Jin et al. 2024; Xiong et al. 2023). It has been found that NK-exo can deliver perforin and granzyme to target cells through endocytosis (Alturani et al. 2024; Lin et al. 2022; Zhao et al. 2022). Moreover, NK-exo plays a pivotal role in reducing immune suppression, modulating the tumor immune microenvironment, and promoting tumor growth through caspase-dependent and caspase-independent cell death pathways (Ghaedrahmati et al. 2023; Hatami et al. 2023; Kim et al. 2022). These findings present innovative approaches to addressing the limitations of NK cell-based therapies for solid tumors. However, little is known of NK-exo effects in pancreatic tumors.

In this study, exosomes were isolated from NK cells derived from UCB using ultracentrifugation. Their impact on proliferation, migration, invasion, colony formation, ROS production, and MMP activation in human pancreatic cancer cells were evaluated in both cellular and animal models. This study aims to elucidate the regulatory effects and underlying mechanisms of NK-exo in pancreatic cancer, providing a reference for the use of exosomes in preventing and treating cancer.

2 Materials and methods

2.1 Animals and tissue samples

Four-week-old female BALB/c nude mice weighing (18–22 g) were acquired from Jinan Pengyue Laboratory Animal Breeding Co., Ltd with animal production license no.SCXK-Lu- 2022–0006. Animal assays were performed in accordance with Experimental Animal Care Guidelines. Mice were caged in groups of five in the SPF animal facility under a 12-h light/dark cycle at a constant temperature of 23–25 °C and 35 ± 5% humidity. The animals were acclimatized for 7 days prior to experimentation and euthanized using carbon dioxide (CO_2) inhalation before tissue collection (Brown et al. 2021). All animal experiments were conducted following protocols approved by the Animal Welfare and Ethics Committee of Jining Medical University (Approval No. JNMC- 2024-DW- 293). Umbilical cord blood samples collection were approved by the Ethics Committee of Augie Medical Laboratory Co., Ltd. of Rizhao City (approval no. AJYX- 2023-XB- 01) following the Declaration of Helsinki. All patients provided written informed consent for study participation.

2.2 Cell culture

Ficoll density gradients were used for the isolation of mononuclear cells which were then grown under 5% CO_2 at 37℃ in Lymphocyte Serum-Free Medium KBM581 (88581 CM, Corning) supplemented with 5% platelet lysate (HPCFD-CRL50, AventaCell) and 200 IU/mL IL- 2 (125 ALa, Shuanglu). The medium was refreshed, and cells were passaged every other day. After 14 days, suspension-grown NK cells were obtained, and their surface markers were analyzed via flow cytometry (BDCantoII, USA) by following a previously described protocol (Bradley et al. 2018). Human PANC- 1 cells were procured from the Collection of Authenticated Cell Cultures and cultured in DMEM (11,965, Gibco) supplemented with 10% fetal bovine serum (10,091,148, Gibco) at 37 °C with 5% CO_2.

2.3 Exosome isolation

The exosome purification method used in the present study has been previously described by Mrowczynski et al. (2018). The culture supernatant was collected from cells grown in serum-free media for 48 h. The supernatant underwent sequential centrifugation at 4 °C under the following conditions: 3,000 × g for 15 min, 10,000 × g for 30 min, and 100,000 × g for 60 min. The precipitate was filtered (0.45 μm) and centrifuged at 100,000 × g for 60 min, followed by resuspension of the pellet in chilled PBS and storage at − 80 °C for further use. The total protein concentration of the NK-exo was quantified by a BCA Protein Assay Kit (P0010S, Beyotime) following the manufacturer's protocol, and adjusted to 1.0 mg/mL using sterile PBS prior to use.

2.4 Nanoparticle tracking and analysis

The size distribution and concentration of NK-exo particles were assessed using a Zetaview-PMX120-Z system (Particle Metrix, Germany) and ZetaView software (version 8.05.14 SP7) as demonstrated in a previous study (Zheng et al. 2013).

2.5 Transmission electron microscopy (TEM)

The structures of the isolated NK-exo were observed using under TEM (JEM1400, Jeol, Japan). A 20 μL aliquot of exosomal suspension was deposited onto a 200-mesh copper grid (AZH200, Zhongjing) and allowed to stand at ambient temperature for 10 min. The sample was stained with 2%

phosphotungstic acid (A601241, Sangon Biotech) for 3 min and examined following the manufacturer's protocol(Zhang et al. 2021).

2.6 Nano-FCM (nFCM) measurement

The surface biosignature proteins of NK-exo were detected using nano-flow cytometer (nFCM, Tian et al. 2019). Diluted exosomes were stained with FITC-conjugated mouse anti-human CD9 (555,371, BD) and CD81 antibodies (551,108, BD) at room temperature for 30 min, with isotype IgG used as a negative control. Post-incubation, the mixture was washed twice with PBS and centrifuged at 100,000 × g for 60 min. After discarding the supernatant, the pellet was resuspended in 50 µL of cold PBS and analyzed using a nanoanalyzer (N30E, NanoFCM, China).

2.7 Cellular uptake assay

NK-exo were fluorescently labeled with a PKH26 red fluorescence labeling kit (D0030, Solarbio) for 10 min. PANC- 1 cells (4×10^4/well) were inoculated in 24-well plates and grown overnight. Labeled NK-exo were incubated with the PANC- 1 cells for 10 h after ultrafiltration at 10,000 × g for 20 min using a 10 kDa cut-off membrane to remove unbound dye (Xia et al. 2019). The cells were counterstained with Hoechst 33,258 (C0021, Solarbio) and analyzed for uptake.

2.8 Western blot analysis

Cell lysates and exosome pellets were dissolved in ice-cold RIPA buffer (P0013B, Beyotime) for 30 min. Extracted proteins were separated on 10% SDS-PAGE and transferred to PVDF membranes (ISEQ00010, Millipore), followed by blocking with 5% skim milk in TBST for 1 h. The blots were treated overnight with primary antibodies at 4 °C, followed by HRP-conjugated secondary antibodies (Hu et al. 2024). Protein bands were visualized using a chemiluminescence detection system (iBright FL1000, Invitrogen). The antibodies used included those targeting CD81 (1:3000, 41,779, SAB), Calnexin (1:3000, 12,186, SAB), Syntenin (1:3000, ab185832, Abcam), Caspase3 (1:1000, GB11767 C, Servicebio), Caspase9 (1:1000, GB12053, Servicebio), Cyt c (1:1000, GB11080, Servicebio), Bax (1:1000, GB11690, Servicebio), Bcl- 2 (1:1000, GB154830, Servicebio) and GAPDH (1:1000, GB15004, Servicebio).

2.9 CCK- 8 assays

The viability of PANC- 1 cells in the presence of NK-exo was assessed using CCK- 8 assays (CA1210, Solarbio). Cells (5×10^3/well) were inoculated in 96-well plates and grown overnight after which the media were substituted for varying concentrations of NK-exo, followed by the addition of CCK-8 working solution. After a 2-h incubation at 37 °C, absorbance at 450 nm were read in a microplate reader (Multiskan SkyHigh, Thermo Fisher, USA) and applied for cell viability calculation (Liu et al. 2023).

2.10 Apoptosis analysis

The effect of NK-exo on apoptosis in PANC- 1 cells was assessed using FCM and the Annexin V-FITC/PI dual-staining assay using a kit (C1062, Beyotime) as instructed (Wu et al. 2023). PANC- 1 cells (4×10^5 cells/well) were inoculated in 6-well plates and grown with varying concentrations of NK-exo for 48 h. After treatment, cells were collected, stained with Annexin V-FITC/PI solution for 15 min, and analyzed by FCM to determine the apoptosis rate.

2.11 Cell scratch assay

PANC- 1 cells (5×10^5/well) were inoculated in 6-well plates. When confluent, the monolayer was scratched with a 200 µL pipette tip and the movement of cells was evaluated for 48 h. The scratch widths were measured using ImageJ software, and healing rates were calculated to assess migration capacity (Wu et al. 2017).

2.12 Migration and invasion assays

A 24-well Transwell system (3422, Corning) was utilized to evaluate PANC- 1 cell migration and invasion as previously described (Jiang et al. 2023). For invasion, 60 µL of Matrigel (1:10 dilution in serum-free media; CLS354234, Sigma) was applied to the upper chamber. Starved PANC- 1 cells (2×10^4 in 200 µL serum-free media) were introduced to the upper compartment, while the lower compartment contained 500 µL DMEM supplemented with 20% FBS and varying concentrations of NK-exo. After 48 h, migrating and invading cells were fixed with 4% paraformaldehyde (P1110, Solarbio), stained with 1% crystal violet (C8470, Solarbio), and counted using an inverted microscope (IX73P2 F, Olympus, Japan).

2.13 Colony formation assays

PANC- 1 cells (2×10^3/well) were inoculated in 6-well plates and grown overnight before treatment with varying amounts of NK-exo for 48 h. The media were then substituted for NK-exo-free media, and cells were grown for 10 days to allow colony formation. The colonies were fixed and stained as above and quantified (Reza et al. 2016).

2.14 ROS detection

Intracellular ROS levels were assessed using a ROS Assay Kit with DCFH-DA (S0033, Beyotime) (Ko et al. 2014). PANC- 1 cells (4×10^5/well) were grown in 6-well plates or confocal dishes () for 48 h and divided into four groups: control (PBS), N-acetylcysteine (NAC; 0.6 µmol/mL, 616,911, Sigma), NK-exo (50 µg/mL), and NAC + NK-exo (0.6 µmol/mL NAC + 50 µg/mL NK-exo). After 48 h of further growth, cells in confocal dishes were stained with DCFH-DA for 20 min and analyzed using a confocal laser microscope (Leica STELLARIS5, Germany). Cells in 6-well plates were harvested, stained with DCFH-DA, and analyzed using FCM.

2.15 MMP assay

The MMP assays were performed using a JC- 1 assay kit (C2003S, Beyotime). PANC − 1 cells (4×10^5/well) were grown for 48 h in either 6-well plates or confocal dishes. Cells were divided into four groups: control (PBS), NAC (0.6 µmol/mL), NK-exo (50 µg/mL), and NAC + NK-exo (0.6 µmol/mL NAC + 50 µg/mL NK-exo). After 48 h, cells in the confocal dishes were stained with JC- 1 solution for 20 min and visualized using a confocal laser microscope. Cells in the 6-well plates were harvested, stained with JC- 1, and analyzed via FCM (De Bortoli et al. 2018).

2.16 qRT-PCR

PANC- 1 cells (4×10^5 cells/well) were inoculated in 6-well plates and grown with varying concentrations of NK-exo for 48 h. qRT-PCR was performed as described previously (Zhu et al. 2023). Total RNA was extracted from PANC- 1 cells using the MiniBEST Universal RNA Extraction Kit (9767, Takara). cDNA synthesis was performed using the PrimeScript RT reagent Kit (RR047 A, Takara). Amplification was conducted with a Bio-Rad Real-Time PCR system (CFX96, Bio-rad, USA) with TB Green Premix Ex Taq II (RR820L, Takara), and results were normalized to GAPDH. Relative gene expression was determined using the $2^{-\Delta\Delta Ct}$ method. Primer sequences are provided in Supplement Table 1.

2.17 *In vivo* tumor formation assay

To evaluate the anti-tumor effects of NK-exo on pancreatic tumors, PANC- 1 cells (2×10^6/mouse) in 200 µL PBS were injected subcutaneously into the right flanks of the 4-week-old BALB/c nude mice. Once the tumor volumes reached approximately 30 mm^3, the mice were randomly allocated into three groups (n = 10) and administered weekly intratumoral injections of either 3.0 mg of NK-exo protein (2.07×10^{12} particles) or 5.0 mg of NK-exo protein (3.45×10^{12} particles) in a volume of 100 µL of PBS per kilogram of body weight over a duration of two weeks (Klapproth et al. 2020). At the end of the treatment, the mice were euthanized, and the tumors were subsequently weighed and photographed for further analysis.

2.18 Immunohistochemistry

Following the excision of tumor xenografts, immunohistochemical staining was conducted as described in reference (Liu et al. 2022). To examine Bax expression in PANC- 1 tumor tissues, samples measuring 1 × 1 × 1 cm were excised, fixed in 4% paraformaldehyde, and subsequently processed into 5 µm paraffin-embedded sections. Antigen retrieval was performed using citrate buffer (P0086, Beyotime) for 15 min via standard microwave heating. Sections were blocked with 5% BSA (SW3015, Solarbio) for 1 h, followed by overnight incubation at 4 °C with an anti-Bax-PARP antibody (1:500, GB11690, Servicebio). Tissues were then incubated with HRP-conjugated secondary antibodies (GB23301, Servicebio) for 1 h and counterstained with hematoxylin (G1120, Solarbio) for 30 s. Sections were examined under an Olympus optical microscope (BX53, Olympus), and data were analyzed using ImageJ software.

2.19 Data collection and statistical analysis

To ensure accuracy and reproducibility, all experiments were conducted by investigators who were blinded to the group assignments, and each experiment was performed in triplicate. All data are presented as mean ± SD. Statistical analysis was conducted using GraphPad Prism version 9.0. Differences between the two groups were analyzed with an unpaired two-tailed Student's *t*-test, while comparisons among multiple groups were performed using a one-way analysis of variance (ANOVA) followed by Tukey's post hoc test. *P* values < 0.05 were considered statistically significant. Significance levels are denoted as follows: ns, not significant; $^*P < 0.05$; $^{**}P < 0.01$; $^{***}P < 0.001$; $^{****}P < 0.0001$.

3 Results

3.1 Isolation and characterization of NK cells

UCB-derived NK cells were cultured in suspension and aggregation in vitro, displaying round or oval shapes (Supplement Fig. 1 A). FCM analysis revealed that 88.18% of the cells expressed CD56, 75.79% expressed CD16, and 75.42% were double-positive for both markers, consistent with typical human NK cell characteristics (Supplement Fig. 1B). These findings confirmed the suitability of these cells for preparing NK-exo from UCB.

3.2 Isolation and identification of NK-exo

TEM demonstrated that NK-exo exhibit a characteristic cup-shaped bilayer membrane vesicle structure (Fig. 1A). The diameter and particles concentration of NK-exo were 122.7 nm and 7.65 $\times 10^{11}$ particles/mL, respectively (Fig. 1B). Western blot analysis confirmed the enrichment of exosomal markers, including CD81 and Syntenin, and the absence of the endoplasmic reticulum marker Calnexin (Fig. 1C). nFCM analysis revealed that 4.4% and 57.2% of NK-exo were positive for CD9 and CD81, respectively (Fig. 1D). Confocal microscopy detected red fluorescence from PKH26-labeled NK-exo inside PANC- 1 cells, indicating successful internalization of NK-exo through endocytosis (Fig. 1E).

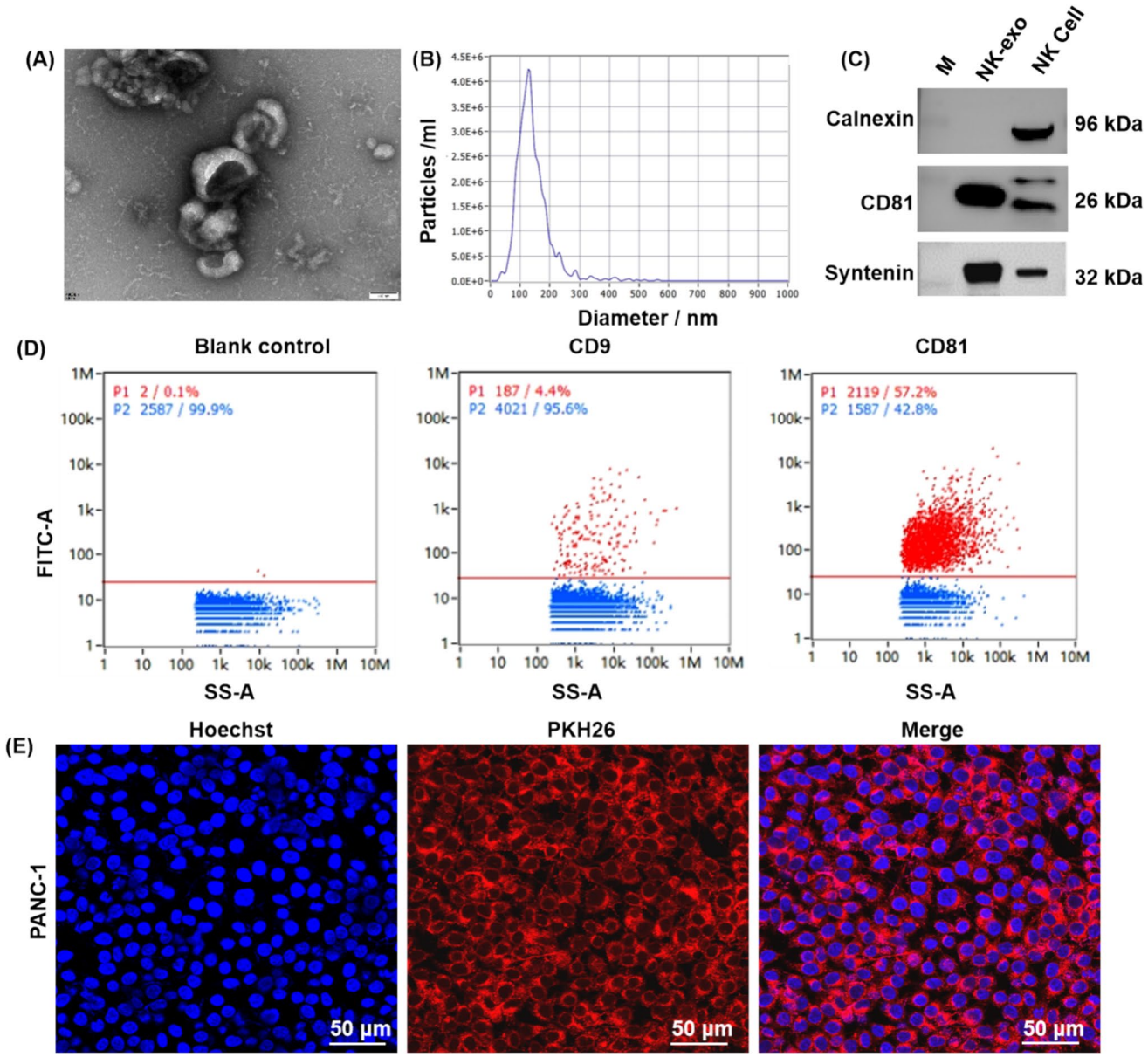

Fig. 1 Identification of NK-exo **A**. Morphological examination of NK-exo under an electron microscope, displaying characteristic exosomal features. **B**. Nanoparticle tracking analysis was employed to determine the particle concentration and size distribution of NK-exo. **C**. Western blots showing presence of exosomal markers (CD81 and Syntenin) and the lack of the negative marker Calnexin. **D**. Nano-flow cytometry analysis showing the positive rates of CD9 and CD81 on NK-exo. **E**. Internalization of NK-exo by PANC- 1 cells, visualized using the red fluorescent dye PKH26

3.3 NK-exo modulate viability and apoptosis in PANC- 1 cells

The impact of NK-exo on cell viability was assessed using CCK- 8 assays. PANC- 1 cells were treated with varying NK-exo concentrations (0, 10, 30, 50, 100 μg/mL) for 24 and 48 h, revealing significant, dose- and time-dependent reductions in viability. After 24 h, viability decreased notably compared to the control, with the effect becoming more pronounced over time. At 100 μg/mL for 48 h, cell viability dropped to 33.43%, indicating a strong inhibitory effect of NK-exo on PANC- 1 cell survival (Fig. 2A). Annexin V/PI staining demonstrated that treatment with NK-exo significantly and dose-dependently induced apoptosis (Fig. 2B), as evidenced by an increase in the total apoptosis rate from 3.59% in the control group to 39.89% in the 50 μg/mL treatment group (Fig. 2C).

3.4 NK-exo suppress tumorigenic behavior

To assess the effects of NK-exo on cellular migration, invasion, and colony formation capabilities, wound healing, transwell, and colony formation assays were performed (Fig. 3A-D). PANC- 1 cells exhibited a significant, dose-dependent decrease in these capabilities relative to the control group. Notably, the closure rate in the 50 μg/mL treatment group was 19.96%, in contrast to 80.60% observed in the control group after 48 h (Fig. 3E). Furthermore, the number of PANC- 1 cells traversing the membrane was significantly reduced in the high-dose NK-exo group (116.12, 54.6) compared to the control group (32.67, 19.2), as illustrated in Fig. 3F and G, respectively. Co-culture with NK-exo for 48 h resulted in a marked reduction in PANC- 1 colonies, with the 50 μg/mL group exhibiting 60.33 colonies compared to 328.67 in the control group (Fig. 3H).

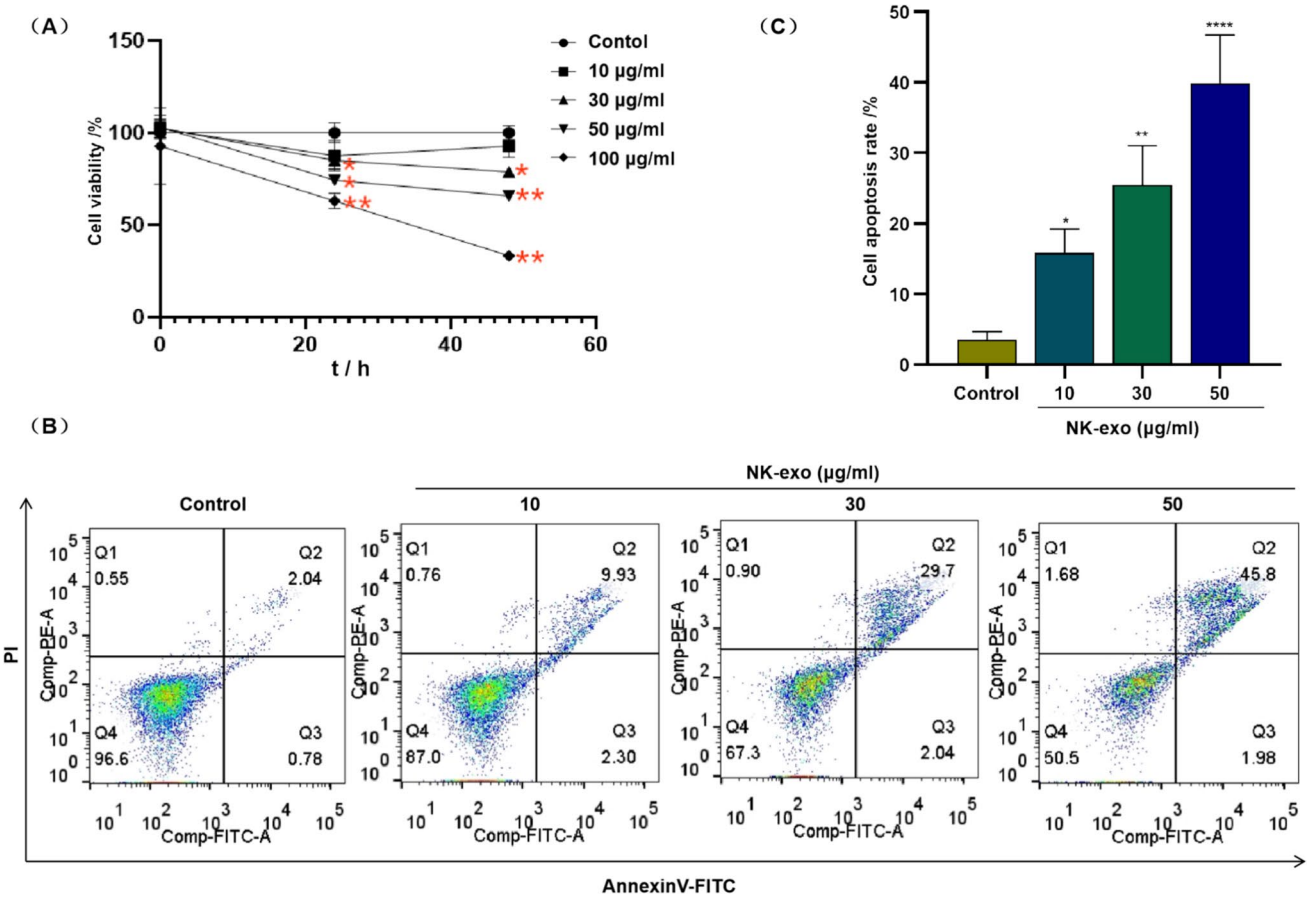

Fig. 2 NK-exo modulates viability and promotes apoptosis in PANC-1 cells **A**. The statistical analysis of the CCK- 8 assay results indicated a reduction in PANC- 1 cell viability in the NK-exo treatment groups at concentrations of 30, 50, and 100 μg/mL (*$P < 0.05$, **$P < 0.01$ vs control, n = 4). **B**. The flow cytometry analysis illustrates the apoptosis levels in PANC- 1 cells across various experimental groups. **C**. The statistical analysis of cells apoptosis levels showed that the NK-exo treatment was significantly increased the apoptosis rate of NK-exo (*$P < 0.05$, **$P < 0.01$, ***$P < 0.001$ vs control, n = 3). All results are represented as means ± S.D. by ANOVA

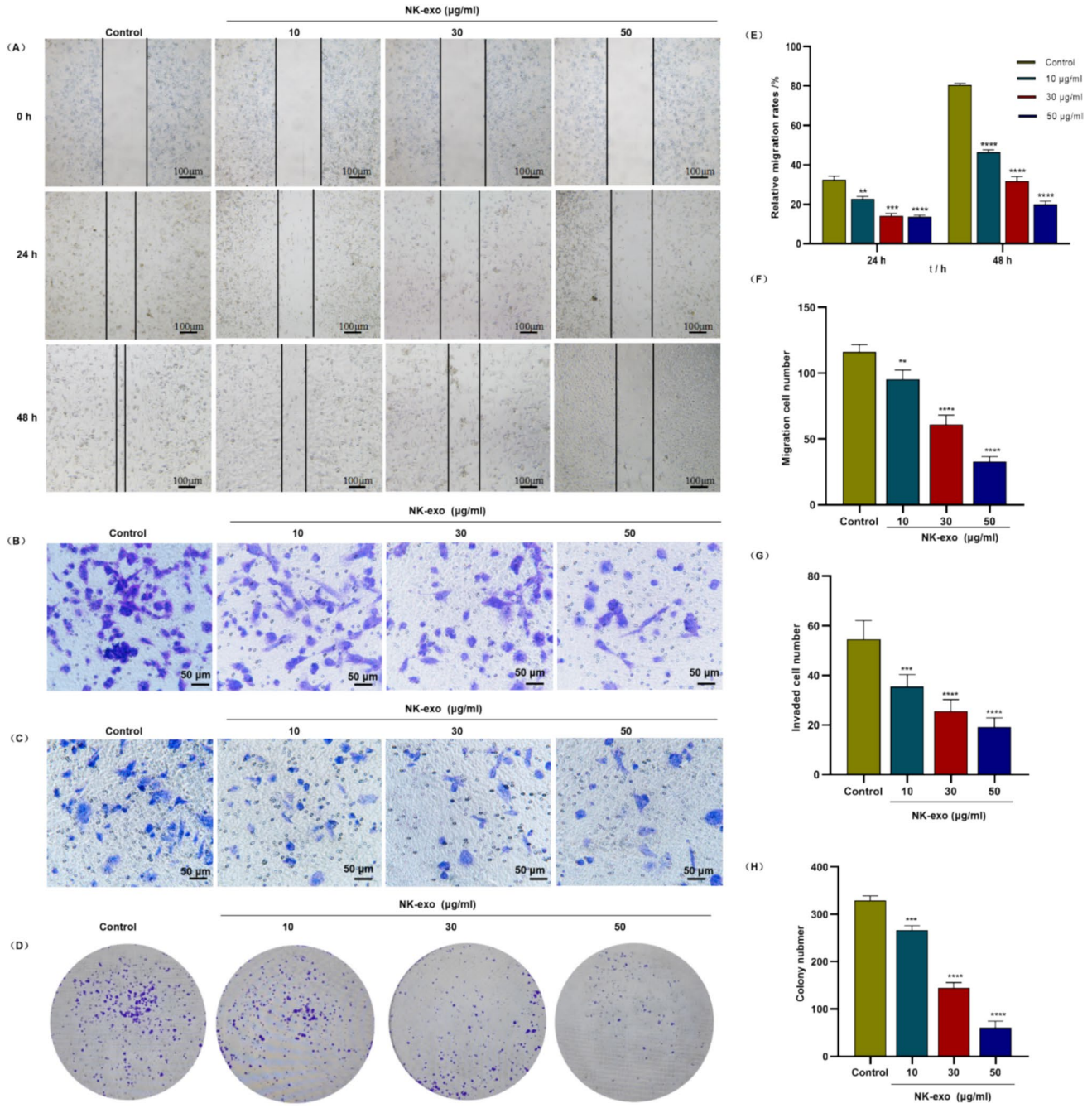

Fig. 3 NK-exo inhibits tumorigenic behavior of PANC- 1 cells **A**. Scratch cell assay showing reduced migration of PANC- 1 cells treated with NK-exo. **B**. Transwell assays showing the effects of NK-exo on cell migration. **C**. Transwell assays illustrating decreased invasive capacity of PANC- 1 cells treated with NK-exo. **D**. Colony formation assay showing significant reduction in colony formation in NK-exo treated PANC- 1 cells. **E–H**. A quantitative analysis of the migration rate and the number of migrating or invading PANC-1 cells revealed a significant, dose-dependent reduction after treated with NK-exo for 48 h (**$P < 0.01$, ***$P < 0.001$, ****$P < 0.0001$ vs control, n = 3). All results are represented as means ± S.D. by ANOVA

3.5 NK-exo triggers mitochondrial apoptosis by modulating ROS and MPP levels

The intracellular levels of ROS and MMP were quantitatively assessed using DCFH-DA and JC- 1 fluorescent probes, respectively, after a 48-h treatment with NK-exo, NAC, or a combination of both (Fig. 4A, B). FCM analysis demonstrated a substantial increase in ROS fluorescence intensity in PANC- 1 cells treated with NK-exo (10,887.25) compared to the control group (6,067.67), that was notably

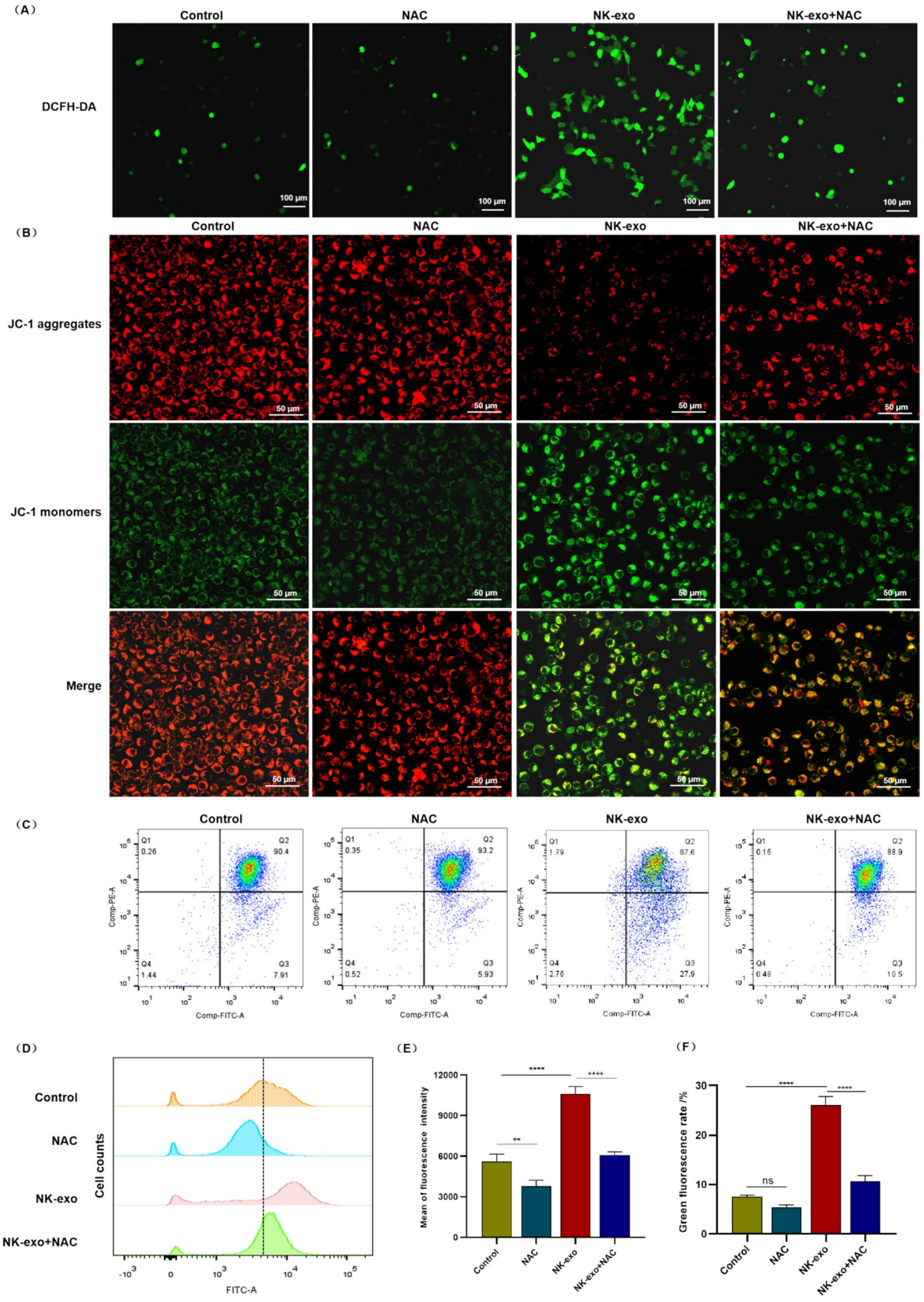
(A)
Control
NAC
NK-exo
NK-exo+NAC
DCFH-DA
100 μm
(B)
JC-1 aggregates
JC-1 monomers
Merge
50 μm
(C)
Q1 0.26
Q2 90.4
Q4 1.44
Q3 7.91
Q1 0.35
Q2 93.2
Q4 0.52
Q3 5.93
Q1 1.79
Q2 67.6
Q4 2.76
Q3 27.9
Q1 0.16
Q2 88.9
Q4 0.48
Q3 10.5
Comp-PE-A
Comp-FITC-A
(D)
Cell counts
FITC-A
(E)
Mean of fluorescence intensity
(F)
Green fluorescence rate /%
ns

◂**Fig. 4** NK-exo significantly increas ROS levels and reduce MMP in PANC- 1 cells **A**. ROS levels in PANC- 1 cells were measured using DCFH-DA as a probe and visualized via confocal microscopy. **B**. MMP in PANC- 1 cells was assessed using JC- 1 staining, with fluorescence intensities captured by confocal microscopy. **C**. Flow cytometry analysis quantified changes in MMP across experimental groups. **D**. Mitochondrial ROS increase in PANC- 1 cells was validated through flow cytometry. E. Statistical analysis demonstrated a substantial increase in ROS fluorescence intensity in PANC- 1 cells treated with NK-exo (****$P < 0.0001$ vs control, n = 3), that was notably diminished in the NAC + NK-exo treatment group (****$P < 0.0001$ vs NK-exo, n = 3). F. Statistical analysis revealed an significantly increase in MMP level in the NK-exo group (****$P < 0.0001$ vs control, n = 3), with a diminished effect was noted in the NAC + NK-exo group (****$P < 0.0001$ vs NK-exo, n = 3). Results are presented as mean ± S.D. by ANOVA

diminished to 6,582.39 in the NAC + NK-exo treatment group (Fig. 4E), as evidenced by a rightward shift in the cell population peaks (Fig. 4D). Simultaneously, JC- 1 probes demonstrated a significant decrease in red fluorescence and an increase in green fluorescence within PANC- 1 cells, indicative of mitochondrial depolarization (Fig. 4B). This observation was corroborated by FCM analysis (Fig. 4C), which revealed an over threefold increase in the NK-exo group (26.07) compared to the control group (7.51), with a significantly diminished effect was noted in the NAC + NK-exo group (10.69), as illustrated in Fig. 4F.

3.6 Effect of NK-exo on apoptosis-associated proteins

qRT-PCR analysis revealed significant elevations in the apoptotic markers *Caspase- 3* (2.02-fold) and Caspase- 9 (2.42-fold) following treatment with 50 μg/mL NK-exo, relative to the control group. Conversely, treatment with NK-exo resulted in a substantial reduction in the expression levels of genes associated with mitochondrial biogenesis, specifically *PGC- 1α* (0.50-fold), *TFAM* (0.06-fold), and *SOD2* (0.58-fold), as depicted in Fig. 5A. The expression changes in PANC- 1 cells following NK-exo treatment were confirmed by Western blotting analysis (Fig. 5B). Results revealed a concentration-dependent decrease in the anti-apoptotic Bcl- 2, with a marked increase in the pro-apoptotic Caspase3, Caspase9, Bax, and Cyt c ($P < 0.01$), as illustrated in Fig. 5C. This shows that NK-exo modulates mitochondrial biogenesis and oxidative metabolism, potentially through the PGC- 1α-TFAM axis, thereby enhancing apoptosis in PANC- 1 cells.

3.7 NK-exo promote PANC- 1 cell xenograft growth *in vivo*

Xenograft transplantation in murine models was performed to assess the inhibitory effects of NK-exo on the in vivo proliferation of PANC- 1 cells (Fig. 6A). Analysis of tumor regression demonstrated markedly reduced tumor sizes and weight in the 3 mg/kg (1.10 mm^3, 0.99 g) or 5 mg/kg (0.58 mm^3, 0.52 g) NK-exo treated group relative to the controls (1.74 mm^3, 1.42 g), as illustrated in Fig. 6B. Immunohistochemical analysis using ImageJ software indicated a substantial, concentration-dependent increase in Bax levels in the animals treated with 3 mg/kg (55.42%) or 5 mg/kg (68.19%) compared to control group (37.76%), as illustrated in Fig. 6C and D. These results further verify the pro-apoptotic and anti-tumor effects of NK-exo in an in vivo pancreatic cancer model.

4 Discussion

In recent years, the role of NK cell-derived exosomes in various diseases has garnered significant scholarly attention, underscoring the therapeutic potential of these nanoparticles (Razizadeh et al. 2023). In this study, we isolated activated NK cells and revealed that NK-exo exert cytotoxic effects on pancreatic tumor cells by inducing ROS-mediated mitochondrial dysfunction. These findings elucidate the antitumor activity of NK-exo and suggest their potential as a novel and natural therapeutic agent for cancer treatment.

Pancreatic cancer, often referred to as the "king of cancers", remains a significant global health concern due to its increasing incidence and high mortality rates. According to the American Cancer Association, pancreatic cancer ranked as the second leading cause of digestive malignancy-related deaths in 2022, claiming approximately 50,000 lives in the United States alone (Stoffel et al. 2023). Pancreatic ductal adenocarcinoma, responsible for over 80% of pancreatic cancer cases, has gained attention for its challenging intervention strategies (Bogdanski et al. 2024). Despite advances, the mechanisms driving pancreatic cancer onset and progression remain incompletely understood. Therefore, there is a pressing need to investigate potential therapeutic strategies for pancreatic cancer.

Recent developments in tumor immunology have positioned immunotherapy as a potential treatment for pancreatic cancer, with NK cells playing a vital role in this therapy (Lee et al. 2019; Vivier et al. 2024). Nevertheless, NK cells within pancreatic tumors exhibit diminished cytotoxic activity and reduced interferon-gamma (IFN-γ) expression, while paradoxically producing elevated levels of the immunosuppressive cytokine interleukin- 10 (IL- 10) (Marcon et al. 2020). A progressive decline in NK cell activity has been observed as pancreatic cancer advances (Lee et al. 2021). NK-exo in addition to retaining the tumor cell killing function of NK cells, also have the characteristics of high safety, wide source, easy to preserve and transport (Zhu et al. 2017, 2018). Nevertheless, a limited number of studies have

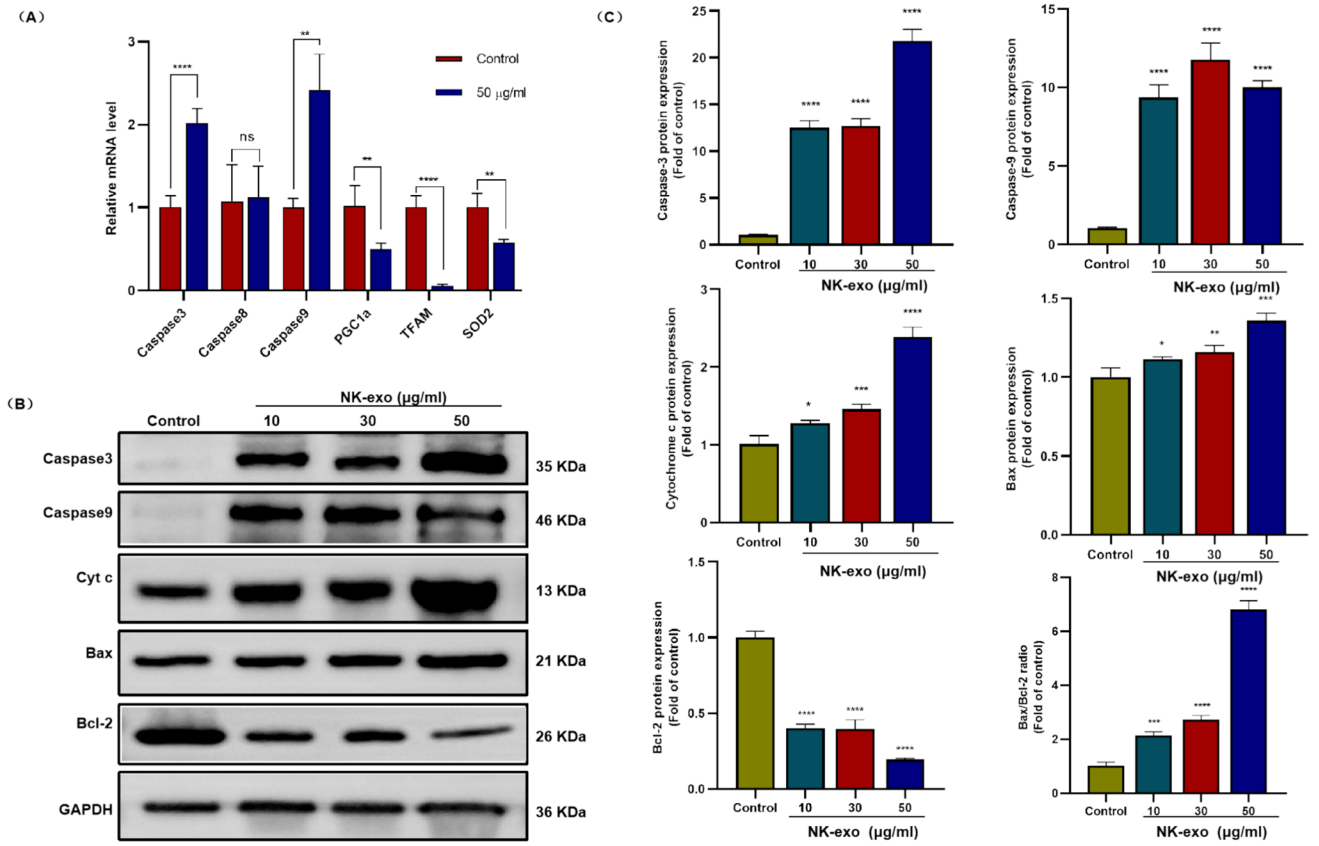

Fig. 5 Modulation of apoptosis-associated genes in PANC- 1 cells by NK-exo **A**. qRT-PCR analysis of mRNA expression levels for *Caspase3* (****$P < 0.0001$ vs control, n = 4), *Caspase8* (ns, no significance vs control, n = 4), *Caspase9* ($P = 0.0086$ vs control, n = 4), *PGC- 1α* ($P = 0.0064$ vs control, n = 4), *TFAM* (****$P < 0.0001$ vs control, n = 4), and *SOD2* ($P = 0.0021$ vs control, n = 4) in PANC-1 cells, normalized to GAPDH. **B**. Western blots showing Caspase3, Caspase9, Cyt c, Bax, and Bcl- 2 levels in PANC- 1 cells. **C**. Protein quantification was conducted for Caspase3, Caspase9, Cyt c, Bax, and Bcl- 2 in PANC- 1 cells following a 48-h treatment with NK-exo (*$P < 0.05$, **$P < 0.01$, ***$P < 0.001$, ****$P < 0.0001$ vs control, n = 3). Results are presented as mean ± S.D. by ANOVA

specifically investigated the effects and mechanisms of NK-exo on pancreatic cancer.

In this study, we successfully isolated and cultured a substantial quantity of natural killer (NK) cells derived from umbilical cord blood (UCB). Our ex vivo expansion technique markedly enhanced the population of $CD16^+CD56^+$ NK cells from an initial progenitor population characterized by low CD16 or CD56 expression, increasing the proportion of $CD3^+CD56^+$ NK cells from 2.56% to 75.42%. These results are consistent with findings reported in prior research (Vasu et al. 2015). In our study, exosomes derived from UCB NK cells exhibited similar shape, size, and marker characteristics to NK-exo reported in previous research (Li et al. 2020). Moreover, we initially demonstrated the internalization of NK-exo by PANC- 1 cells in vitro, which was a crucial step for NK-exo to exert their anti-tumor effects. To investigate the effects of NK-exo on PANC- 1 cells, we assessed cell viability, migration, invasion, colony formation, and apoptosis in vitro after co-culturing PANC- 1 cells with varying concentrations of NK-exo. For the first time, to our knowledge, the findings revealed that NK-exo could significantly inhibit the tumorigenic properties of PANC-1 cells in a dose- and time-dependent manner. However, the anti-tumor mechanisms of NK-exo remain largely unexplored.

Recent research by Pan et al. has demonstrated that reactivated NK cells can induce the loss of mitochondrial outer membrane potential and rapidly trigger the release of cytochrome c from mitochondria in both blood and solid cancer cell lines, suggesting that induction of mitochondrial apoptosis may be a general mechanism for NK-mediated killing (Pan et al. 2022). Concurrently, recent studies have identified the increased production of reactive oxygen species (ROS) as a critical factor in the progression of pancreatic cancer, primarily by facilitating apoptosis through mitochondrial pathways (Nunnari and Suomalainen 2012; Wang et al. 2021; Wen et al. 2022). Therefore, we hypothesize that NK-exo may inhibit pancreatic tumor growth by targeting mitochondrial dysfunction. We further examined the intracellular MMP and ROS production of PANC- 1 cells

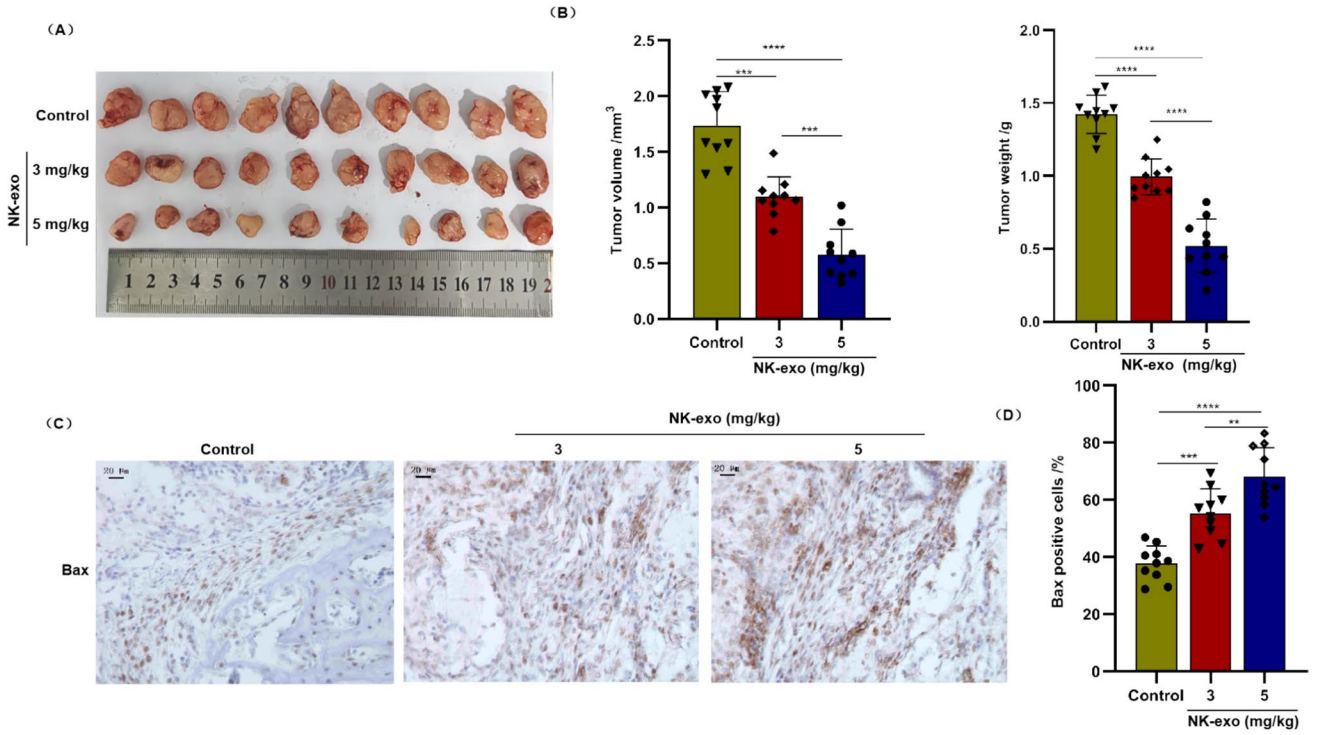

Fig. 6 NK-exo inhibits the proliferation of transplanted PANC- 1 cell xenograft tumors in mice **A**. photographic evidence of tumor development in xenograft-transplanted nude mouse models across different experimental groups. **B**. Quantitative analysis confirms a significant reduction in tumor size and weight with 3 mg/kg or 5 mg/kg NK-exo injection (***$P < 0.001$, ****$P < 0.0001$ vs control, n = 10). **C**. IHC analysis of Bax in tumors of different groups. **D**. Statistical analysis revealed a significant upregulation of Bax expression induced by NK-exo (**$P < 0.01$, ***$P < 0.001$, ****$P < 0.0001$ vs control, n = 10). Results are presented as mean ± S.D. by ANOVA

after treated with NK-exo. Our findings revealed that NK-exo significantly increased ROS levels and decreased MMP. The addition of NAC, a synthetic precursor to intracellular cysteine and glutathione (Xu et al. 2024), indicated that NK-exo may inhibit pancreatic cancer progression by inducing excessive ROS accumulation, that are consistent with previous research findings and offering a potential therapeutic intervention.

Previous studies have established PGC- 1α as a key regulator of mitochondrial biogenesis and oxygen consumption (Abu Shelbayeh et al. 2023; Xue et al. 2023). However, the mechanisms by which NK-exo influences mitochondrial function remain unexplored. We further investigates whether *PGC- 1α* and mitochondrial biogenesis are implicated in NK-exo induced tumor apoptosis. qRT-PCR was utilized to evaluate the expression levels of *PGC- 1α*, *TFAM*, and *SOD2* in cells treated with NK-exo. The findings reveal that NK-exo suppresses the PGC- 1α/TFAM mitochondrial biogenesis pathway, as evidenced by the downregulation of *PGC- 1α* and *TFAM*, both of which are critical regulators of mitochondrial biogenesis. Furthermore, *SOD2*, known for its protective role against oxidative damage, was also downregulated. This downregulation may be a pivotal mechanism leading to the activation of *caspase- 3* and *caspase- 9* in PANC- 1 cells, as depicted in Fig. 5A. Western blot analysis corroborated these findings, revealing dose-dependent elevations in Caspase- 3 and Caspase- 9 protein activity, as well as an increased Bax/Bcl- 2 ratio, which is a hallmark of apoptosis due to its regulatory role in cytochrome c release (Jedram et al. 2023), indicative of apoptotic processes. In vivo experiments further substantiated these results, demonstrating significantly elevated Bax expression in tumors treated with NK-exo. Collectively, the findings of this study suggest that NK-exo may inhibit the progression of pancreatic cancer by enhancing mitochondrial oxidative damage via the PGC- 1α/TFAM-induced caspase pathway.

While these findings provide promising insights, additional research is required to elucidate the mechanisms by which the NK-exo induces mitochondrial dysfunction and apoptosis in pancreatic cancer through *PGC- 1α/TFAM* pathway. Furthermore, it is imperative to replicate the experimental work presented in this study across a more diverse array of pancreatic cancer cell lines. Such efforts would serve to validate the findings and enhance the robustness of the proposed conclusions.

5 Conclusion

This study elucidates the role and underlying mechanisms of NK-exo in the inhibition of pancreatic cancer progression, as well as to explore their potential therapeutic applications. Experimental results indicate that NK-exo derived from umbilical cord blood significantly affects the mitochondrial function of pancreatic cancer cells. This effect is manifested by a decrease in MMP and an increase in the accumulation of ROS. These changes lead to mitochondrial dysfunction, which in turn induces apoptosis in pancreatic cancer cells, as evidenced by decreased cell viability, an increased rate of apoptosis, elevated expression levels of intracellular apoptosis-related proteins, reduced capabilities for cell migration and invasion, diminished clonogenic potential, and weakened in vivo growth. These findings highlight the potential of NK-exo derived from UCB NK cells as a promising immunotherapeutic strategy for pancreatic cancer, providing a novel perspective on its application in oncological treatment. Further research and development are required to assess the therapeutic efficacy and mechanisms of NK-exo in clinical applications.

Supplementary Information The online version contains supplementary material available at https://doi.org/10.1007/s44446-025-00009-3.

Acknowledgements The authors wish to extend their sincere appreciation to Litao Zhang and Shanshan Zhang for their kind assistance.

Author's contribution Data curation, Dongjun Jiang and Feng Zhu; Funding acquisition, Yanqun Wu; Methodology, Yanyun Zheng, Xinfeng Zou, and Qun Li; Validation, Yanyun Zheng, Xinfeng Zou, and Qun Li; Writing – original draft, Yanqun Wu; Writing–review & editing, Dongjun Jiang and Feng Zhu. All authors have read and agreed to the published version of the manuscript.

Funding This study was supported by the Research Fund for Academician LinHe New Medicine Programme (JYHL2022MS20), the Small and Medium Sized Enterprise Innovation Capability Enhancement Project of Shandong Province (2023TSGC0549), the Key Research and Development Program of Rizhao City (2023ZDYF010144), the Research Project on Experimental Teaching and Teaching Laboratory Development of Jining Medical University (SY2024011), College Students' Innovative Entrepreneurial Training Plan Program(202410443016).

Data availability The original contributions presented in the study are included in the article/supplementary material, further inquiries can be directed to the corresponding author.

Declarations

Ethical approval The animal study was approved by Animal Welfare and Ethics Committee of Jining Medical University (approval no.: JNMC- 2024-DW- 293 on 16 July 2024). The study was conducted in accordance with the local legislation and institutional requirements. The studies involving humans were approved by the Ethics Committee of Augie Medical Laboratory Co., Ltd. of Rizhao City (approval no.: AJYX- 2023-XB- 01 on 21 September 2023). The studies were conducted in accordance with the local legislation and institutional requirements. The participants provided their written informed consent to participate in this study. No potentially identifiable images or data are presented in this study.

Competing interests The authors declare no competing or conflicting interests.

References

Abu Shelbayeh O, Arroum T, Morris S, Busch KB (2023) PGC-1α is a master regulator of mitochondrial lifecycle and ROS stress response. Antioxidants (Basel) 12:1075. https://doi.org/10.3390/antiox12051075

Alturani MMAB, Butler AE, Moin ASM (2024) Therapeutic applications of stem cell-derived exosomes. Int J Mol Sci 25:3562. https://doi.org/10.3390/ijms25063562

Bogdanski AM, van Hooft JE, Boekestijn B, Bonsing BA, Wasser MNJM, Klatte DCF, van Leerdam ME (2024) Aspects and outcomes of surveillance for individuals at high-risk of pancreatic cancer. Fam Cancer 23:323–339. https://doi.org/10.1007/s10689-024-00368-1

Bradley T, Peppa D, Pedroza-Pacheco I, Li D, Cain DW, Henao R, Venkat V, Hora B, Chen Y, Vandergrift NA, Overman RG, Edwards RW, Woods CW, Tomaras GD, Ferrari G, Ginsburg GS, Connors M, Cohen MS, Moody MA, Borrow P, Haynes BF (2018) RAB11FIP5 expression and altered natural killer cell function are associated with induction of HIV broadly neutralizing antibody responses. Cell 175:387–399. https://doi.org/10.1016/j.cell.2018.08.064

Brown CW, Chhoy P, Mukhopadhyay D, Karner ER, Mercurio AM (2021) Targeting prominin2 transcription to overcome ferroptosis resistance in cancer. EMBO Mol Med 13(8):e13792. https://doi.org/10.15252/emmm.202013792

Chen CW, Wang LL, Zaman S, Gordon J, Arisi MF, Venkataraman CM, Chung JJ, Hung G, Gaffey AC, Spruce LA, Fazelinia H, Gorman RC, Seeholzer SH, Burdick JA, Atluri P (2018) Sustained release of endothelial progenitor cell-derived extracellular vesicles from shear-thinning hydrogels improves angiogenesis and promotes function after myocardial infarction. Cardiovasc Res 114:1029–1040. https://doi.org/10.1093/cvr/cvy067

De Bortoli M, Taverna E, Maffioli E, Casalini P, Crisafi F, Kumar V, Caccia C, Polli D, Tedeschi G, Bongarzone I (2018) Lipid accumulation in human breast cancer cells injured by iron deplectors. J Exp Clin Cancer Res 37:75. https://doi.org/10.1186/s13046-018-0737-z

Ghaedrahmati F, Esmaeil N, Abbaspour M (2023) Targeting immune checkpoints: how to use natural killer cells for fighting against

solid tumors. Cancer Commun (Lond) 43:177–213. https://doi.org/10.1002/cac2.12394
Hatami Z, Hashemi ZS, Eftekhary M, Amiri A, Karpisheh V, Nasrollahi K, Jafari R (2023) Natural killer cell-derived exosomes for cancer immunotherapy: innovative therapeutics art. Cancer Cell Int 23:157. https://doi.org/10.1186/s12935-023-02996-6
Hosseini R, Sarvnaz H, Arabpour M, Ramshe SM, Asef-Kabiri L, Yousefi H, Akbari ME, Eskandari N (2022) Cancer exosomes and natural killer cells dysfunction: biological roles, clinical significance and implications for immunotherapy. Mol Cancer 21:15. https://doi.org/10.1186/s12943-021-01492-7
Hu W, Kuang X, Zhang Y, Luo Y, Zhang L (2024) Neuroprotective effects of phenylacetylglycine via β2AR on cerebral ischemia/reperfusion injury in rats. Saudi Pharm J 32:102210. https://doi.org/10.1016/j.jsps.2024.102210
Jedram O, Maphanao P, Karnchanapandh K, Mahalapbutr P, Thanan R, Sakonsinsiri C (2023) Corosolic acid induced apoptosis via upregulation of Bax/Bcl-2 Ratio and Caspase-3 activation in cholangiocarcinoma cells. ACS Omega 9:1278–1286. https://doi.org/10.1021/acsomega.3c07556
Jiang M, Jike Y, Liu K, Gan F, Zhang K, Xie M, Zhang J, Chen C, Zou X, Jiang X, Dai Y, Chen W, Qiu Y, Bo Z (2023) Exosome-mediated miR-144-3p promotes ferroptosis to inhibit osteosarcoma proliferation, migration, and invasion through regulating ZEB1. Mol Cancer 22:113. https://doi.org/10.1186/s12943-023-01804-z
Jin X, Zhang J, Zhang Y, He J, Wang M, Hei Y, Guo S, Xu X, Liu Y (2024) Different origin-derived exosomes and their clinical advantages in cancer therapy. Front Immunol 15:1401852. https://doi.org/10.3389/fimmu.2024.1401852
Kim HY, Min HK, Song HW, Yoo A, Lee S, Kim KP, Park JO, Choi YH, Choi E (2022) Delivery of human natural killer cell-derived exosomes for liver cancer therapy: an in vivo study in subcutaneous and orthotopic animal models. Drug Deliv 29:2897–2911. https://doi.org/10.1080/10717544.2022.2118898
Klapproth AP, Shevtsov M, Stangl S, Li WB, Multhoff G (2020) A new pharmacokinetic model describing the biodistribution of intravenously and intratumorally administered Superparamagnetic Iron Oxide Nanoparticles (SPIONs) in a GL261 xenograft glioblastoma model. Int J Nanomedicine 15:4677–4689. https://doi.org/10.2147/IJN.S254745
Ko E, Jeong D, Kim J, Park S, Khang G, Lee D (2014) Antioxidant polymeric prodrug microparticles as a therapeutic system for acute liver failure. Biomaterials 35:3895–3902. https://doi.org/10.1016/j.biomaterials.2014.01.048
Lee J, Kang TH, Yoo W, Choi H, Jo S, Kong K, Lee SR, Kim SU, Kim JS, Cho D, Kim J, Kim JY, Kwon ES, Kim S (2019) An antibody designed to improve adoptive NK-Cell therapy inhibits pancreatic cancer progression in a murine model. Cancer Immunol Res 7:219–229. https://doi.org/10.1158/2326-6066.CIR-18-0317
Lee HS, Leem G, Kang H, Jo JH, Chung MJ, Jang SJ, Yoon DH, Park JY, Park SW, Song SY, Bang S (2021) Peripheral natural killer cell activity is associated with poor clinical outcomes in pancreatic ductal adenocarcinoma. J Gastroenterol Hepatol 36:516–522. https://doi.org/10.1111/jgh.15265
Li D, Wang Y, Jin X, Hu D, Xia C, Xu H, Hu J (2020) NK cell-derived exosomes carry miR-207 and alleviate depression-like symptoms in mice. J Neuroinflammation 17:126. https://doi.org/10.1186/s12974-020-01787-4
Lin Z, Wu Y, Xu Y, Li G, Li Z, Liu T (2022) Mesenchymal stem cell-derived exosomes in cancer therapy resistance: recent advances and therapeutic potential. Mol Cancer 21:179. https://doi.org/10.1186/s12943-022-01650-5
Liu Y, Watabe T, Kaneda-Nakashima K, Shirakami Y, Naka S, Ooe K, Toyoshima A, Nagata K, Haberkorn U, Kratochwil C, Shinohara A, Hatazawa J, Giesel F (2022) Fibroblast activation protein targeted therapy using [177Lu]FAPI-46 compared with [225Ac]FAPI-46 in a pancreatic cancer model. Eur J Nucl Med Mol Imaging 49:871–880. https://doi.org/10.1007/s00259-021-05554-2
Liu M, Peng T, Hu L, Wang M, Guo D, Qi B, Ren G, Wang D, Li Y, Song L, Hu J, Li Y (2023) N-glycosylation-mediated CD147 accumulation induces cardiac fibrosis in the diabetic heart through ALK5 activation. Int J Biol Sci 19:137–155. https://doi.org/10.7150/ijbs.77469
Marcon F, Zuo J, Pearce H, Nicol S, Margielewska-Davies S, Farhat M, Mahon B, Middleton G, Brown R, Roberts KJ, Moss P (2020) NK cells in pancreatic cancer demonstrate impaired cytotoxicity and a regulatory IL-10 phenotype. Oncoimmunology 9:1845424. https://doi.org/10.1080/2162402X.2020.1845424
Mrowczynski OD, Madhankumar AB, Sundstrom JM, Zhao Y, Kawasawa YI, Slagle-Webb B, Mau C, Payne RA, Rizk EB, Zacharia BE, Connor JR (2018) Exosomes impact survival to radiation exposure in cell line models of nervous system cancer. Oncotarget 9:36083–36101. https://doi.org/10.18632/oncotarget.26300
Nunnari J, Suomalainen A (2012) Mitochondria: in sickness and in health. Cell 148:1145–1159. https://doi.org/10.1016/j.cell.2012.02.035
Pan R, Ryan J, Pan D, Wucherpfennig KW, Letai A (2022) Augmenting NK cell-based immunotherapy by targeting mitochondrial apoptosis. Cell 185:1521–1538. https://doi.org/10.1016/j.cell.2022.03.030
Razizadeh MH, Zafarani A, Taghavi-Farahabadi M, Khorramdelazad H, Minaeian S, Mahmoudi M (2023) Natural killer cells and their exosomes in viral infections and related therapeutic approaches: where are we? Cell Commun Signal 21:261. https://doi.org/10.1186/s12964-023-01266-2
Ren S, Chen J, Guo J, Liu Y, Xiong H, Jing B, Yang X, Li G, Kang Y, Wang C, Xu X, Liu Z, Zhang M, Xiang K, Li C, Li Q, Machens HG, Chen Z (2022) Exosomes from adipose stem cells promote diabetic wound healing through the eHSP90/LRP1/AKT axis. Cells 11:3229. https://doi.org/10.3390/cells11203229
Reza AMMT, Choi YJ, Yasuda H, Kim JH (2016) Human adipose mesenchymal stem cell-derived exosomal-miRNAs are critical factors for inducing anti-proliferation signalling to A2780 and SKOV-3 ovarian cancer cells. Sci Rep 6:38498. https://doi.org/10.1038/srep38498
Sordo-Bahamonde C, Lorenzo-Herrero S, Payer ÁR, Gonzalez S, López-Soto A (2020) Mechanisms of apoptosis resistance to NK cell-mediated cytotoxicity in cancer. Int J Mol Sci 21:3726. https://doi.org/10.3390/ijms21103726
Stoffel EM, Brand RE, Goggins M (2023) Pancreatic cancer: Changing epidemiology and new approaches to risk assessment, early detection, and prevention. Gastroenterology 164:752–765. https://doi.org/10.1053/j.gastro.2023.02.012
Tian Y, Gong M, Hu Y, Liu H, Zhang W, Zhang M, Hu X, Aubert D, Zhu S, Wu L, Yan X (2019) Quality and efficiency assessment of six extracellular vesicle isolation methods by nano-flow cytometry. J Extracell Vesicles 9:1697028. https://doi.org/10.1080/20013078.2019.1697028
Vasu S, Berg M, Davidson-Moncada J, Tian X, Cullis H, Childs RW (2015) A novel method to expand large numbers of CD56(+) natural killer cells from a minute fraction of selectively accessed cryopreserved cord blood for immunotherapy after transplantation. Cytotherapy 17:1582–1593. https://doi.org/10.1016/j.jcyt.2015.07.020
Vivier E, Rebuffet L, Narni-Mancinelli E, Cornen S, Igarashi RY, Fantin VR (2024) Natural killer cell therapies. Nature 626:727–736. https://doi.org/10.1038/s41586-023-06945-1
Wang F, Wang L, Qu C, Chen L, Geng Y, Cheng C, Yu S, Wang D, Yang L, Meng Z, Chen Z (2021) Kaempferol induces ROS-dependent apoptosis in pancreatic cancer cells via TGM2-mediated Akt/mTOR signaling. BMC Cancer 21:396. https://doi.org/10.1186/s12885-021-08158-z

Wen C, Ruan Q, Li Z, Zhou X, Yang X, Xu P, Akuetteh PDP, Xu Z, Deng J (2022) Corynoxine suppresses pancreatic cancer growth primarily via ROS-p38 mediated cytostatic effects. Br J Cancer 127:2108–2117. https://doi.org/10.1038/s41416-022-02002-2

Wu LL, Wen CY, Hu J, Tang M, Qi CB, Li N, Liu C, Chen L, Pang DW, Zhang ZL (2017) Nanosphere-based one-step strategy for efficient and nondestructive detection of circulating tumor cells. Biosens Bioelectron 94:219–226. https://doi.org/10.1016/j.bios.2017.03.009

Wu Y, Shen S, Chen J, Ni W, Wang Q, Zhou H, Chen J, Zhang H, Mei Z, Sun X, Shen P, Jie Z, Xu W, Hong Z, Ma Y, Wang K, Wan S, Wu H, Xie Z, Qin A, Fan S (2023) Metabolite asymmetric dimethylarginine (ADMA) functions as a destabilization enhancer of SOX9 mediated by DDAH1 in osteoarthritis. Sci Adv 9:eade5584. https://doi.org/10.1126/sciadv.ade5584

Xia Y, Zhang G, Han C, Ma K, Guo X, Wan F, Kou L, Yin S, Liu L, Huang J, Xiong N, Wang T (2019) Microglia as modulators of exosomal alpha-synuclein transmission. Cell Death Dis 10:174. https://doi.org/10.1038/s41419-019-1404-9

Xiong S, Tan X, Wu X, Wan A, Zhang G, Wang C, Liang Y, Zhang Y (2023) Molecular landscape and emerging therapeutic strategies in breast cancer brain metastasis. Ther Adv Med Oncol 15:17588359231165976. https://doi.org/10.1177/17588359231165976

Xu C, Chen Y, Zhou Z, Yan Y, Fu W, Zou P, Ni D (2024) ML385, an Nrf2 inhibitor, synergically enhanced celastrol triggered endoplasmic reticulum stress in lung cancer cells. ACS Omega 9:43697–43705. https://doi.org/10.1021/acsomega.4c06152

Xue J, Zhang J, Zhang J, Liu J, Wang F, Li K, Liu C (2023) The Parkinson's disease-associated mutation LRRK2 G2385R alters mitochondrial biogenesis via the PGC-1α-TFAM pathway. Mitochondrion 73:10–18. https://doi.org/10.1016/j.mito.2023.09.002

Yu Y (2023) The Function of NK Cells in Tumor Metastasis and NK Cell-Based Immunotherapy. Cancers (Basel) 15:2323. https://doi.org/10.3390/cancers15082323

Zhang J, Zhang Y, Ma Y, Luo L, Chu M, Zhang Z (2021) Therapeutic potential of exosomal circRNA derived from synovial mesenchymal cells via targeting circEDIL3/miR-485-3p/PIAS3/STAT3/VEGF functional module in rheumatoid arthritis. Int J Nanomedicine 16:7977–7994. https://doi.org/10.2147/IJN.S333465

Zhang Y, Liu Y, Liu J, Liu T, Xiong H, Li W, Fu X, Zhou F, Liao S, Fang L, Liang B (2023) Case report: Preliminary response to tislelizumab plus S-1 in patients with metastatic gallbladder carcinoma: A report of five cases and a literature review. Front Immunol 14:1144371. https://doi.org/10.3389/fimmu.2023.1144371

Zhao Y, Liu T, Zhou M (2022) Immune-cell-derived exosomes for cancer therapy. Mol Pharmaceutics 19:3042–3056. https://doi.org/10.1021/acs.molpharmaceut.2c00407

Zheng Y, Campbell EC, Lucocq J, Riches A, Powis SJ (2013) Monitoring the Rab27 associated exosome pathway using nanoparticle tracking analysis. Exp Cell Res 319:1706–1713. https://doi.org/10.1016/j.yexcr.2012.10.006

Zheng X, Hou Z, Qian Y, Zhang Y, Cui Q, Wang X, Shen Y, Liu Z, Zhou Y, Fu B, Sun R, Tian Z, Huang G, Wei H (2023) Tumors evade immune cytotoxicity by altering the surface topology of NK cells. Nat Immunol 24:802–813. https://doi.org/10.1038/s41590-023-01462-9

Zhu L, Kalimuthu S, Gangadaran P, Oh JM, Lee HW, Baek SH, Jeong SY, Lee SW, Lee J, Ahn BC (2017) Exosomes derived from natural killer cells exert therapeutic effect in melanoma. Theranostics 7:2732–2745. https://doi.org/10.7150/thno.18752

Zhu L, Oh JM, Gangadaran P, Kalimuthu S, Baek SH, Jeong SY, Lee SW, Lee J, Ahn BC (2018) Targeting and therapy of glioblastoma in a mouse model using exosomes derived from natural killer cells. Front Immunol 9:824. https://doi.org/10.3389/fimmu.2018.00824

Zhu C, Xie Y, Li Q, Zhang Z, Chen J, Zhang K, Xia X, Yu D, Chen D, Yu Z, Chen J (2023) CPSF6-mediated XBP1 3'UTR shortening attenuates cisplatin-induced ER stress and elevates chemoresistance in lung adenocarcinoma. Drug Resist Updat 68:100933. https://doi.org/10.1016/j.drup.2023.100933